Fabrication and Characterisation of Magnetorheological Shear Thickening Fluids

Vladimir Sokolovski[1], Tongfei Tian[2]*, Jie Ding[3]* and Weihua Li[1]

[1]School of Mechanical, Materials, Mechatronic and Biomedical Engineering, University of Wollongong, Wollongong, NSW, Australia, [2]School of Science, Technology and Engineering, University of the Sunshine Coast, Sippy Downs, QLD, Australia, [3]Defence Science and Technology Group, Port Melbourne, VIC, Australia

In this article, a magnetorheological shear thickening fluid (MRSTF) was fabricated based on magnetorheological (MR) material and shear thickening fluid (STF). The STF was firstly fabricated as the liquid phase, and carbonyl iron particles were then mixed with the prefabricated STF to synthesise a series of MRSTFs with various iron concentrations. Then, a rheometer was used to measure their viscosities by varying the shear rate under various magnetic fields. Both static and dynamic tests were conducted to study the rheology of MRSTFs under different magnetic fields. The tested results revealed that the MRSTF showed shear thickening under zero magnetic field and MR effect with increasing applied magnetic field. It was also noted that the viscosity of the MRSTFs can be controlled by both shear rate and the applied magnetic field. The concentration of iron particles played an important role in the MRSTFs' rheological properties. The MRSTFs with higher iron particle concentrations revealed lower shear thickening effects but higher MR effects, which means the MRSTF with higher iron concentration can be treated as an effective MR fluid. Meanwhile, the MRSTF with low iron concentration displays good shear thickening effect under weak magnetic field. To summarise the behavior of MRSTFs with various iron concentrations and under different magnetic fields, three regions were proposed to provide guidelines to design MRSTFs and assist in their applications.

Keywords: magnetorheological, shear thickening, fabrication, viscosity, storage modulus, loss modulus

INTRODUCTION

Smart materials and structures have taken a central role in many recent developments of the intelligent materials around the world because of their highly functional and changeable properties in relative applications. The merits of these new intelligent materials include offering optimized performance of existing engineering products, as well as offering new solutions with improved and more robust capabilities (Tian, 2014; Peters et al., 2016; Majumdar et al., 2017). They can be adopted to various client needs in practical structures like sensors and actuators in many engineering, automotive, aerospace, and military applications. Consequently, the field of intelligent materials research has attracted a large number of researchers and significant financial investments in development of new materials designed to enhance and improve every aspect of today's living (Ding et al., 2013; Chen et al., 2017; Avila et al., 2018).

Magnetorheological fluid (MRF) is a type of smart material which consists of ferro particles, carrier fluid, and additives. When the MRF is subjected to a magnetic field, the fluid greatly increases

its apparent viscosity, to the point of becoming a viscoelastic solid. Typical choices of carrier fluid include minerals like silicone oils, polyesters, polyether, synthetic hydrocarbons, and water. MRFs also contain micro-sized ferro magnetic particles which play a key role in the change of their viscosity under applied magnetic field. With no magnetic field present, particles do not exhibit specific orientation and distribute randomly in the carrier fluid, so the apparent viscosity of the fluid remains at low values. When a magnetic field is applied, the particles start to become magnetized and attract each other along the direction of the magnetic flux density forming a gap spanning anisotropic chain-like structure. Eventually, the field-affected fluid will transform into semi-solid state with a large dynamic yield stress of several orders of magnitudes higher than that at zero magnetic field condition, which signals the minimum requirement to make the suspension flow. Generally speaking, good MRFs should exhibit sound saturation magnetization, small coercivity/remnant magnetization, effective MR effect over a wide range of temperature variation, and stability against flocculation and chemical oxidation. The most referred engineering applications of MRFs are MR dampers, which are used in vehicle suspension, civil buildings, and shock absorbers (Dong et al., 2016; Chen and Chen, 2020; Hou and Liu, 2020; Hua et al., 2020).

Shear thickening fluid (STF) is a type of non-Newtonian fluid whose viscosity dramatically increases when it experiences a sudden strike or impact. A common example of STF is a mixture of corn starch and water. It is widely known that a person does not sink into this kind of solution if they run over on it. But they can sink if they stand still or walk over it. STFs are usually made from nanoparticles and carrier liquid. When the shear stress or shear rate is applied, hydroclusters will be formed from the nanoparticles because of collisions with other neighboring nanoparticles, which produces a rapid rise in viscosity. The nanoparticles will even lock together and harden when rapidly struck if the shear stress or shear rate is high enough, and the STF will behave like in a solid state. When the stress is removed or if the shear rate decreases, the material returns to its original fluid-like state (Cossa, 2019).

Because of the unique properties of STFs, they have gained enormous attention around the world, and significant amount of research has been investigated for their applications. Their behavior change has found lots of industrial and commercial applications like dampers, personal protective equipment, and even more in prosthetic limb replacement materials. In the past decade, STFs made from silica nanoparticles loaded in carrier fluids, such as polyethylene glycol, and impregnated in a fabric, have gained attention by military and law enforcement agencies to have potential for usage in liquid body armour and bulletproof vests. The most common application focuses on impregnating Kevlar fabrics with STFs in order to improve its stab resistance and to reduce the number of layers required for maximum penetration resistance (Li et al., 2008; Petel et al., 2015; Wagner and Wetzel, 2007; Grover et al., 2020). STFs can also be used in smart structures due to their unique shear thickening properties (Zhou et al., 2016).

In combining both MRF and STF, novel magnetorheological shear thickening fluid (MRSTF) can be achieved. Zhang et al. (2008) firstly synthesized MRSTF from iron particles and STF at the weight ratios of 5:100, 10:100, 50:100, and 200:100. Then, they investigated the thixotrope of MRSTFs (Zhang et al., 2010). Yang et al. (2015) developed and tested a linear damper working with two MRSTFs which contained 20 and 80% weight fractions of iron particles, respectively. Their results showed the damper with 20% iron displaying both MR effect and shear thickening effect, while the damper with 80% iron worked more like a conventional MR fluid-filled damper, because its shear thickening effect is restrained and the MR effect becomes more obvious with higher iron volume.

In this study, we investigate rheological properties of STFs and MRSTFs, in an effort to present a guideline of three regions of MRSTFs' behavior to apply this novel smart material, which can provide an improved impact performance and dependencies of the MR effect when an external magnetic field is applied. The MRSTFs were fabricated with mixing already prepared STF and carbonyl iron particles. Their dependencies of viscosity/complex viscosity/storage modulus/loss modulus on shear rate and frequency, exposed to various magnetic fields, were tested. The effects of iron particle concentration, magnetic field, and shear rate on rheological properties of the MRSTF were discussed. In order to achieve this again, both steady state and oscillatory tests were conducted. The main objective and motivation of this study was an attempt to first assess the performance of the already developed materials and to try to find ways on how to improve them, and at the same time, researching new techniques that could be of a great importance in various applications. The results of this work, we believe, will create valuable foundation groundwork in determining selection of input materials and quantities to conform with the application requirements, particularly in future improvements in performance and mechanical protection for the applications of MRSTFs (Ding et al., 2011).

MATERIALS AND EXPERIMENTS

Materials and Fabrications

The STF was the base material for MRSTF, and its nano-particles were fumed silica (S5505; Sigma-Aldrich, Germany) with 14 nm primary particles size, 200–300 nm of aggregation size, and a surface area of approximately 200 m^2/g. The carrier fluid was ethylene glycol (102466; Sigma-Aldrich, Germany) with a density of 1.113 g/ml. Compared with the STF made of corn starch and water, the STF made of ethylene glycol and fumed silica has less sedimentation and is more stable (White et al., 2010).
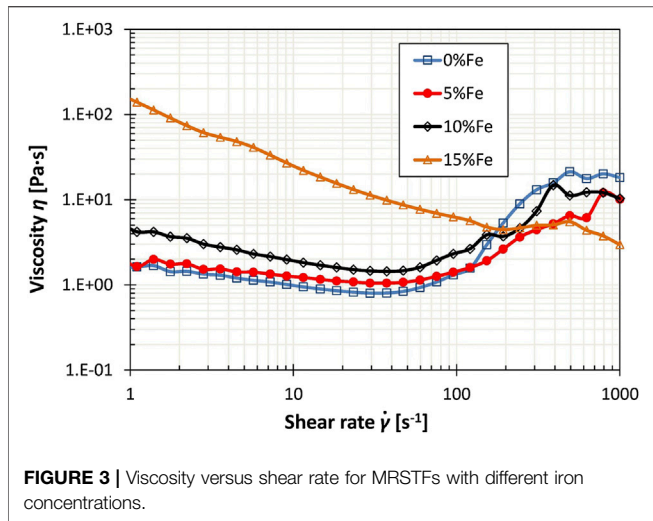
Before the fabrication of STF, fumed silica was put in a beaker and dried in a vacuum oven at a temperature of 100°C for 10 h to evaporate all the moisture out of the material. Then, the carrier fluid was mixed with fumed silica at the weight ratio 3:1, and a blender was employed to mechanically stir the two components until a liquid compound was achieved. Finally, the resulting suspensions were placed in a vacuum chamber for 30 min to eliminate involved air bubbles, and the STF was achieved.

Carbonyl iron particles (C3518; Sigma Aldrich, Germany) were chosen as the ferro particles for the MRSTFs, which have 5 μm particle size and 7.86 g/cm^3 density. The carrier phase was the pre-fabricated STF with 25 wt% fumed silica. For fabrication of MRSTFs, the carbonyl iron particles were mixed with the STF

MRSTF	Ethylene glycol [g]	Fumed silica [g]	Carbonyl iron [g]	Weight fraction of iron (%)
0% Fe	75	25	0	0
5% Fe	75	25	5.26	5
10% Fe	75	25	11.11	10
15% Fe	75	25	17.65	15
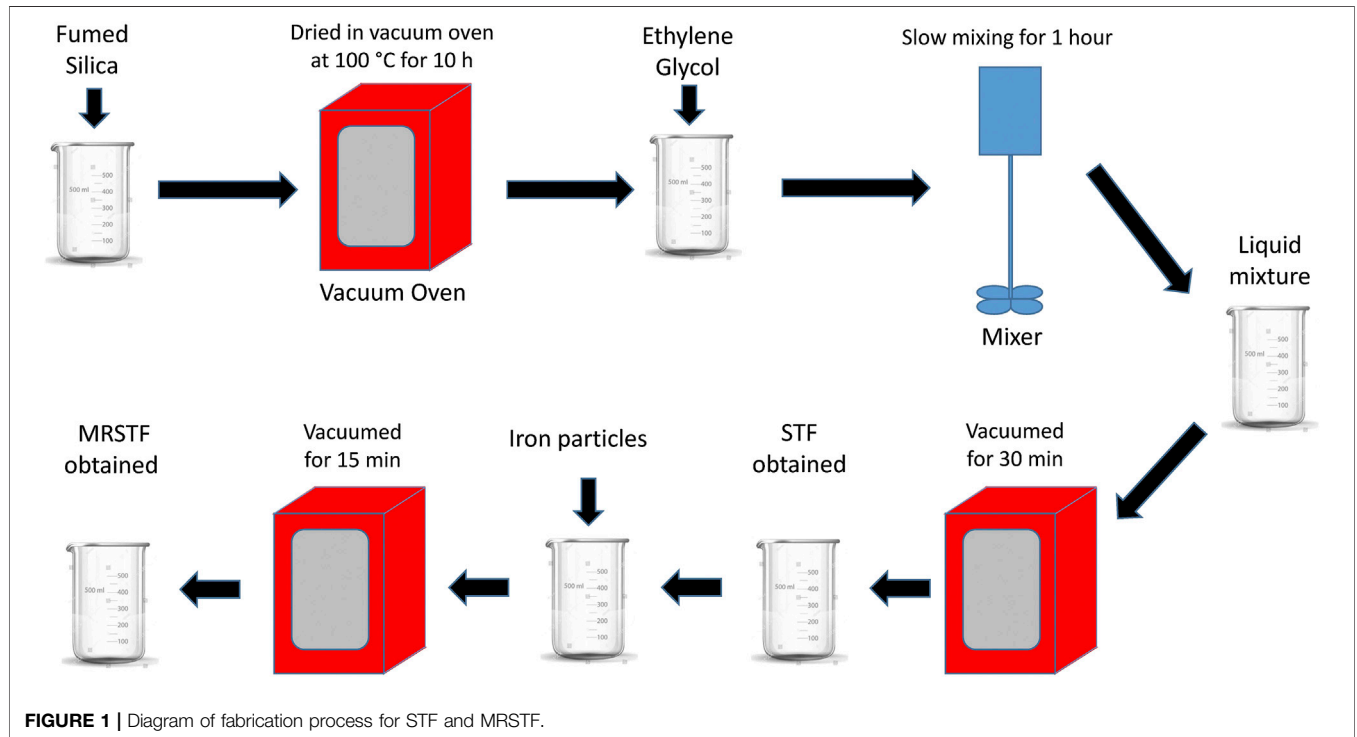
FIGURE 1 | Diagram of fabrication process for STF and MRSTF.
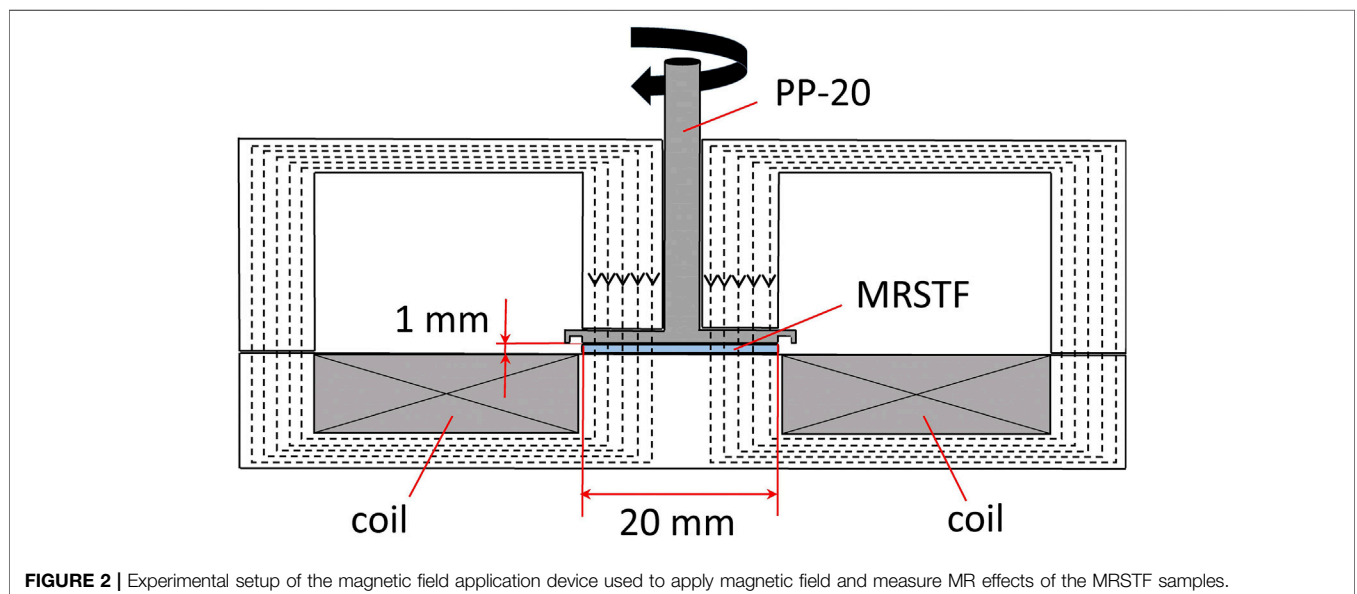
FIGURE 2 | Experimental setup of the magnetic field application device used to apply magnetic field and measure MR effects of the MRSTF samples.

FIGURE 3 | Viscosity versus shear rate for MRSTFs with different iron concentrations.

TABLE 2 | Table representing the ratio between maximum viscosity vs critical viscosity for different concentrations of Fe particles.

MRSTF	Viscosity at the critical shear rate η_c	Maximum viscosity η_{max}	Shear thickening effect η_{max/η_c}
0% Fe	0.80	20.1	25.13
5% Fe	1.05	12.1	11.52
10% Fe	1.44	12.2	8.47
15% Fe	13.35	16.5	1.24

subjecting it to oscillatory shear stress (Han et al., 2016). In the dynamics oscillatory amplitude sweep test, the shear strain amplitude was increased stepwise from 0.01% to 100% while the frequency was maintained at a constant value of 1 Hz. This kind of test was used to describe the behavior of the specimen, by which we can obtain the specimen's limit of the linear viscoelastic region (LVE) as well as its viscoelastic character. In the dynamic oscillatory frequency sweep test, the applied frequency increased stepwise from 0.1 to 100 Hz while keeping the shear strain amplitude constant at 1%. The frequency sweep was generally used to describe the behavior of the samples at slow changes of stress as well as time-dependent behavior of a sample in the nondestructive deformation range.
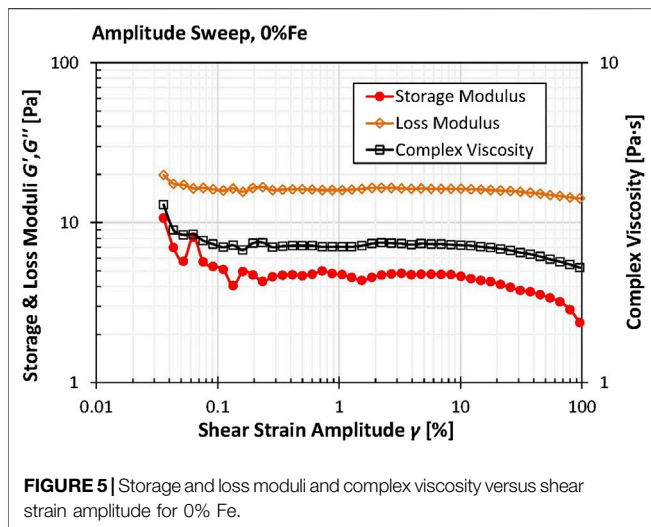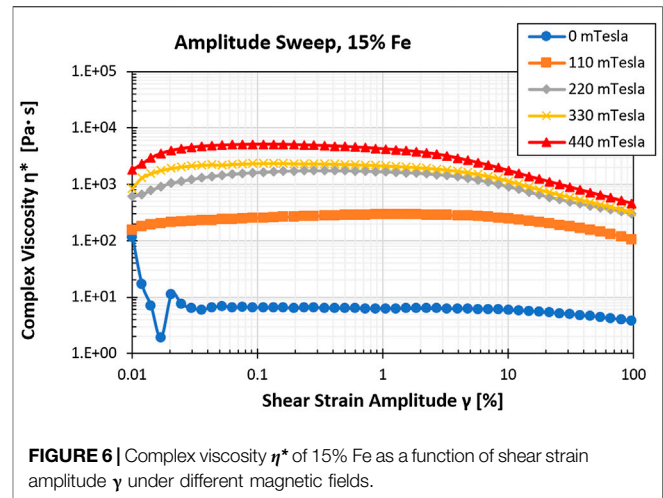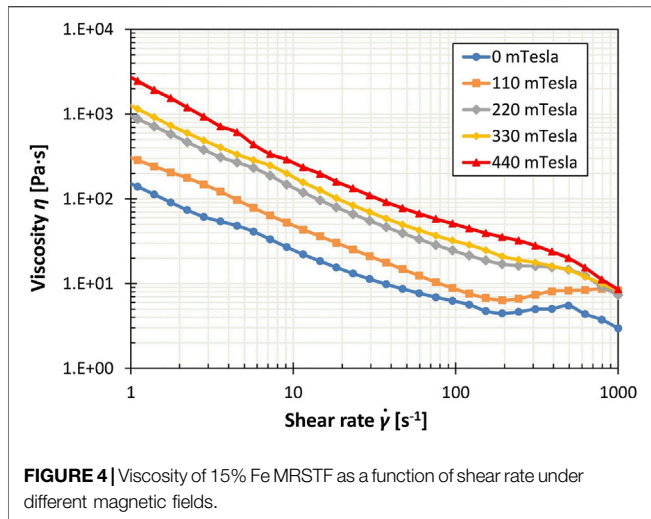
All experimental data were collected using the sensors embedded in the rheometer and transferred simultaneously to a PC, in which the software Rheoplus was used to display the data in both curves and tables. All data were exported from the tables in Rheoplus into Excel and plotted.

Measurements

A rotating rheometer (MCR 301, Anton Paar, Germany) was used to measure the rheological properties of the MRSTFs, and a temperature control device (Viscotherm VT2, Anton Paar, Germany) was used to ensure the measuring temperature at 25°C. A flat measuring geometry (PP-20, Anton Paar, Germany) with 20 mm diameter was used for the rheological testing. Measuring gap of the test was 1 mm. When testing MRSTFs' MR properties with the rheometer, a magnetic induction accessory (MRD180; Anton Paar, Germany) was used to introduce and control the magnetic fields at 0, 110, 220, 330, and 440 mTesla. **Figure 2** shows how the magnetic field is generated and applied to the MRSTF samples in the measurements. The measured data were collected using a rheometer and simultaneously transferred to the PC. A software Rheoplus was used to view the data in the PC screen.

Three types of tests were performed to assess rheological properties of the STF and MRSTF samples, including 1) steady-state test, 2) dynamic oscillatory amplitude sweep test, and 3) dynamic oscillatory frequency sweep test. In a steady-state test, the specimen was rotated isothermally by varying the shear rate from 0.1 to 1,000 s^{-1}, and the viscosity of the sample was measured using the rheometer. For both dynamic oscillatory tests, the specimen was oscillated with controlling the input shear strain amplitude and frequency; meanwhile, the storage and loss moduli and complex viscosity of the specimen were measured. The storage modulus G' represents the elastic property of the viscoelastic behavior of MRSTFs, in which quasi describes the solid-state behavior of the sample. The loss modulus G'' characterizes the viscous portion of the viscoelastic behavior, which can be seen as the liquid-state behavior of the sample. The complex viscosity η^* represents the frequency-dependent viscosity function determined for a viscoelastic fluid by

RESULTS AND ANALYSIS

Steady-State Test

The steady-state test for all MRSTFs was performed where MRSTF samples were rotated isothermally by varying the shear rate from 0.1 to 1,000 s^{-1}. **Figure 3** represents the rheological property of all four MRSTFs at 25°C. It can be observed that for 0% Fe shear rate increase from 1 s^{-1} to the critical shear rate $\dot{\gamma}_c$ (around 30 s^{-1}), a shear thinning behavior is observed, with a local minimum viscosity of $\eta_c = 0.8$ Pa·s. When shear rate increases from critical shear rate to the maximum shear rate $\dot{\gamma}_{max}$ (around 600 s^{-1}), a shear thickening effect is observed with a maximum viscosity of $\eta_{max} = 20.1$ Pa·s. The shear thickening effect of the STF is defined as a ratio between of the maximum viscosity over the viscosity at the critical shear rate $\eta_{max}/\eta_c = 25.13$. With the increase of the iron concentration in MRSTF, the viscosity of MRSTF increases. Meanwhile, the local minimum viscosity of the MRSTF increases, which decreases the shear thickening effect. **Table 2** represents the shear thickening effect of all MRSTFs depending on the iron concentration.

Figure 4 shows the viscosity of 15% Fe versus shear rate under different magnetic fields. It is obvious to see that with the increase of applied magnetic flux density, the viscosity of the sample increases, which is the evidence of the magnetorheological (MR) effect. It is also noted that this MRSTF sample shows a clear shear

FIGURE 4 | Viscosity of 15% Fe MRSTF as a function of shear rate under different magnetic fields.

FIGURE 6 | Complex viscosity $\eta*$ of 15% Fe as a function of shear strain amplitude γ under different magnetic fields.

FIGURE 5 | Storage and loss moduli and complex viscosity versus shear strain amplitude for 0% Fe.

thickening effect without magnetic field, and the shear thickening performance gets weaker when the applied magnetic field is stronger. At 330 and 440 mTesla, the shear thickening effect was not able to be observed as the viscosity of the sample is dominated by the magnetic field. Similar trends have been observed in the MRSTF with 5% Fe and 10% Fe.

Dynamic Oscillatory Amplitude Sweep Test

Dynamic oscillatory amplitude sweep tests were performed where sinusoidal strain amplitude was applied from the range of 0.01 to 100%, while keeping the frequency constant at 1 Hz, at the constant room temperature of 25°C. **Figure 5** shows the storage and loss moduli and complex viscosity versus shear strain amplitude for 0% Fe without magnetic field, which is the base STF without iron particles.

Figure 5 shows that the storage modulus of 0% Fe does not change too much within 10% shear strain amplitude, which indicates that the limit of linear viscoelastic range for the 0% Fe is 10% shear

strain amplitude. The loss modulus and complex viscosity of 0% Fe both stay steady within 20% shear strain amplitude and then slightly decrease with the amplitude increases. The loss modulus of 0% Fe is greater than its storage modulus in the amplitude sweep test, which means the 0% Fe shows a liquid state in this test.

The magnitudes of the magnetic field used in the tests were 0, 110, 220, 330, and 440 mTesla. **Figure 6** shows how the complex viscosity of 15% Fe changes with increasing shear strain amplitude under different magnetic fields.

We can clearly see how complex viscosity increases when stronger magnetic field is applied, which proves the strong MR effect of 15% Fe. This trend has been observed for all three MRSTFs. It is also noted that the under each magnetic field, complex viscosity increases when strain amplitude starts from 0.01% and reaches a plateau value, after which it started to decrease and reached its minimum value when the strain amplitude range approaches 100%.

Figures 7 shows storage and loss moduli of 15% Fe as a function of shear strain amplitude for the range from 0.01 to 100%, respectively. It is evident that each time a stronger magnetic field is applied, both storage and loss moduli increase. This proves the MR effect of MRSTF again. When the applied magnetic field increases from 330 to 440 mTesla, the increase of moduli is relatively smaller than the increase at lower magnetic field, which is due to the saturation of the MRSTFs. For each curve of the storage modulus versus shear strain amplitude, the storage modulus shows a linear range at lower strain amplitudes and decreases after a critical value of the shear strain amplitudes is reached. It is observed that the linear range of storage modulus decreases at a stronger magnetic field. The samples 5% Fe and 10% Fe also had trends similar to the 15% Fe sample.

Dynamic Frequency Oscillation Sweep Testing

Dynamic oscillatory frequency sweep tests were performed where shear strain amplitude was kept constant at 1%, while varying the frequency from 0.1 to 100 Hz, at a constant room temperature of 25°C. In this frequency sweep test, storage and loss moduli and

FIGURE 7 | Storage and loss moduli of 15% Fe as functions of shear strain amplitude under different magnetic fields.
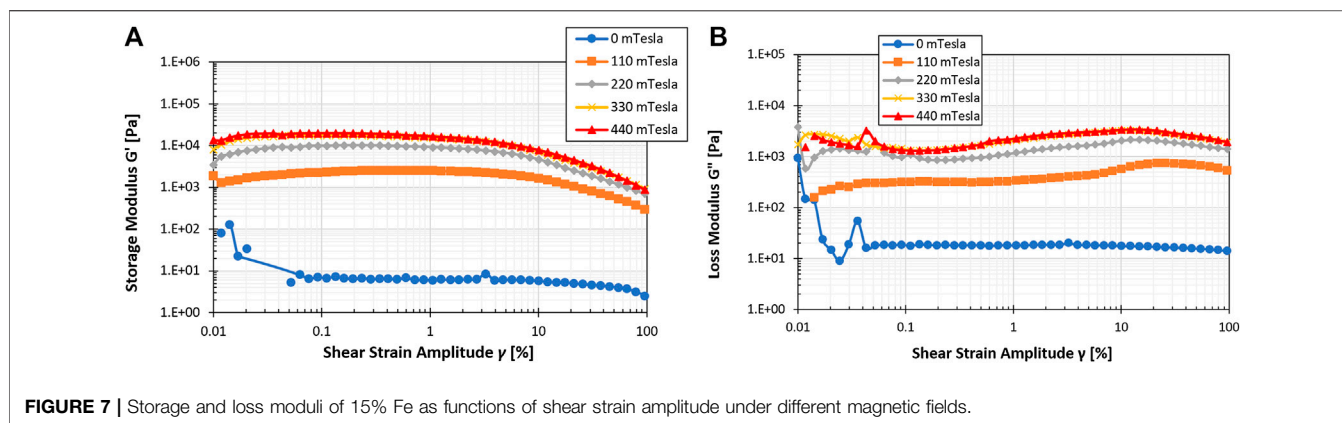
the complex viscosity were measured under different magnetic fields of 0, 110, 220, 330, and 440 mTesla. The complex viscosity of 15% Fe versus frequency under different magnetic fields is shown in **Figure 8**.

With the increase of applied magnetic field, the complex viscosity of 15% Fe has higher values, which is the MR effect due to the iron particles. It is also noted that without magnetic field (0 mTesla), the complex viscosity has an increase region which is between two decrease regions. The increase of complex viscosity is from the base STF which is the evidence of the shear thickening effect. However, when the applied magnetic field gets stronger, the shear thickening effect is weaker and the complex viscosity mainly shows a decrease trend with increase in the frequency. The reason of this phenomenon is the iron particles in MRSTF, which influence the formation of hydro-clusters causing the shear thickening. Consequently, the MRSTF behave more like an MRF when the applied magnetic field is high enough.

Storage and loss modulus were also analysed in the frequency sweep tests, and they are summarized in **Figure 9**.

Figure 9 shows the storage and loss moduli as functions of frequency for the 15% Fe under different magnetic fields. Again, it is evident from the MR effect that each time a stronger magnetic field is applied, the storage and loss moduli both increase. When the applied magnetic field increases from 220 to 440 mTesla, the increment is smaller than that with lower magnetic field.

In **Figure 9a**, it is noted that for each curve, the storage modulus increases with the applied frequency, and the increase trend is stronger at lower magnetic field than the higher magnetic field. In **Figure 9b**, the loss modulus of 15% Fe shows an increase without magnetic field, and it mostly remains constant under an applied magnetic field, which means that the iron particles in MRSTF are greatly affected by the magnetic field. For 5% Fe and 10% Fe, trends were observed to be similar to the 15% Fe.

Comparison Among the Magnetorheological Shear Thickening Fluids

For the steady-state tests performed on the MRSTF with 15% iron content displayed in **Figure 4**, where viscosity is observed as a function of shear rate and different magnetic fields, it can be

**FIGURE 8 |** Complex viscosity η^* as a function of frequency under different magnetic fields.
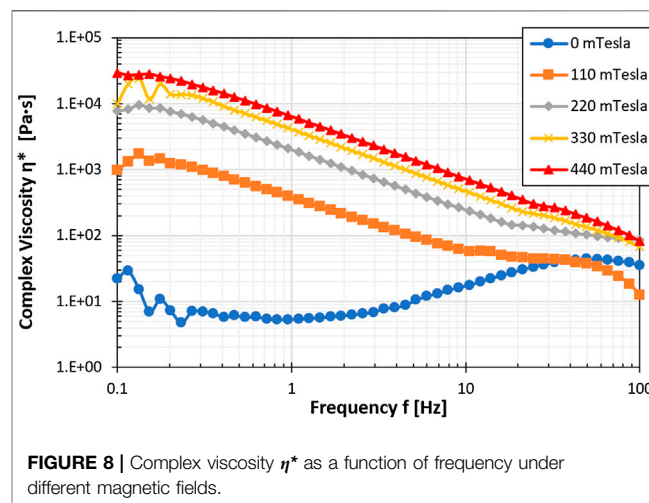
concluded that the increase of iron particle concentration and magnetic field obviously restrain the shear thickening phenomenon. The shear thickening can only be observed at a higher shear rate and zero magnetic field (0 mTesla) or very low magnetic field (110 mTesla). Obviously, with the increase in the magnetic field, the MR effect improved but shear thickening cannot be observed in experiments because of the high concentration of iron particle. When the magnetic field is greater than 220 mTesla, the 15% Fe shows an obvious shear thinning behavior and the viscosity increased with magnetic field strength as expected, i.e., it shows the MR effect like conventional MR fluids.

The shear thickening performance η_{max/η_c} was only recorded for 0 and 110 mTesla in the amounts of: 8/0.928 = 8.62 and 9/6 = 1.5. This proves that the high micron-particle-based MRSTFs have similar behavior to conventional MR fluids.

To assess the magnetorheological and shear thickening behavior of MRSTF, the following graphs are collated to compare the storage and loss moduli as functions of strain amplitude and frequency for all MRSTFs with different iron concentrations.
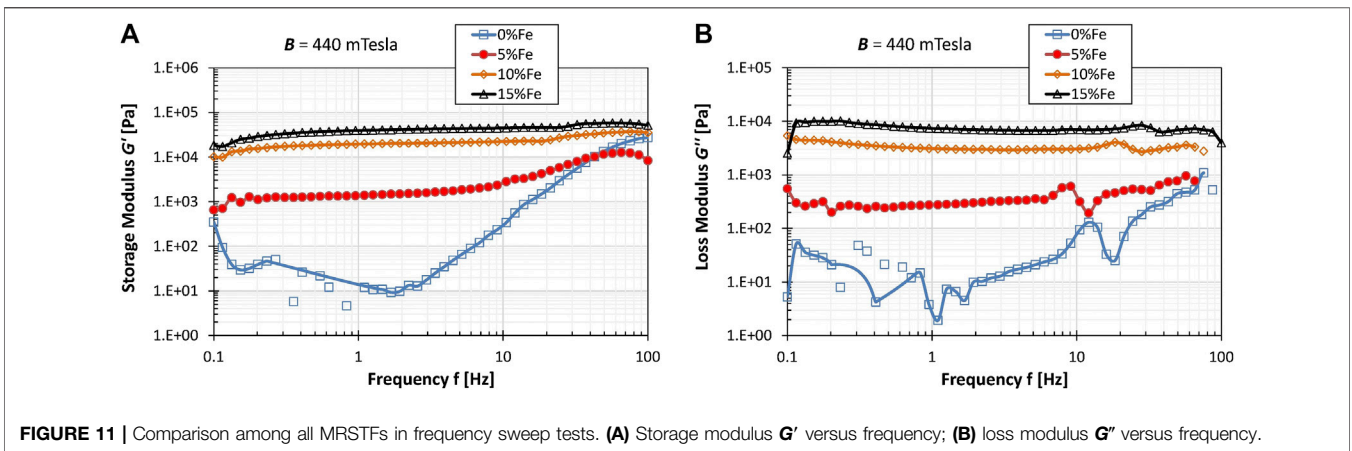
Figures 10 and **11** compare the storage and loss moduli of all four MRSTFs in shear strain sweep tests and frequency sweep at the magnetic field of 440 mTesla, respectively.
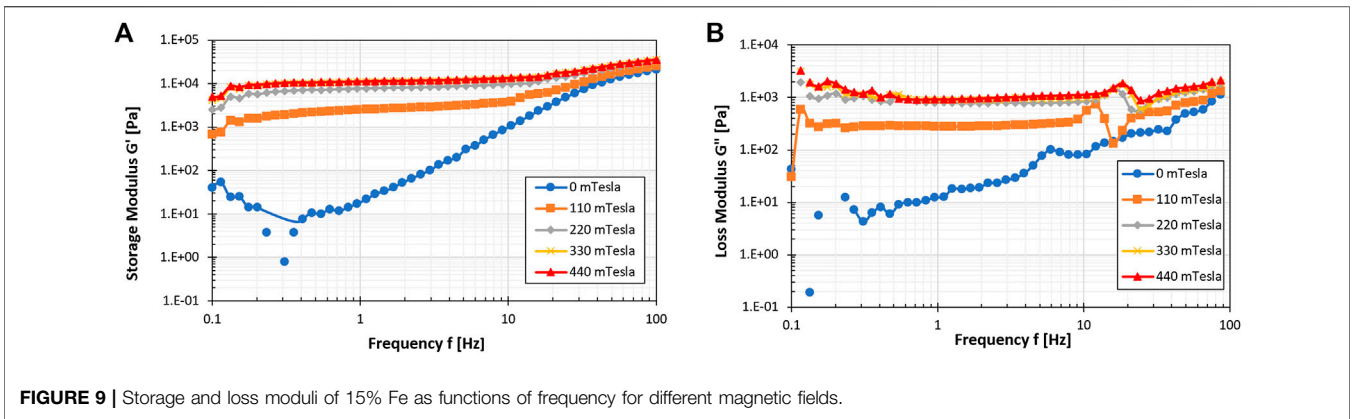
**FIGURE 9 |** Storage and loss moduli of 15% Fe as functions of frequency for different magnetic fields.
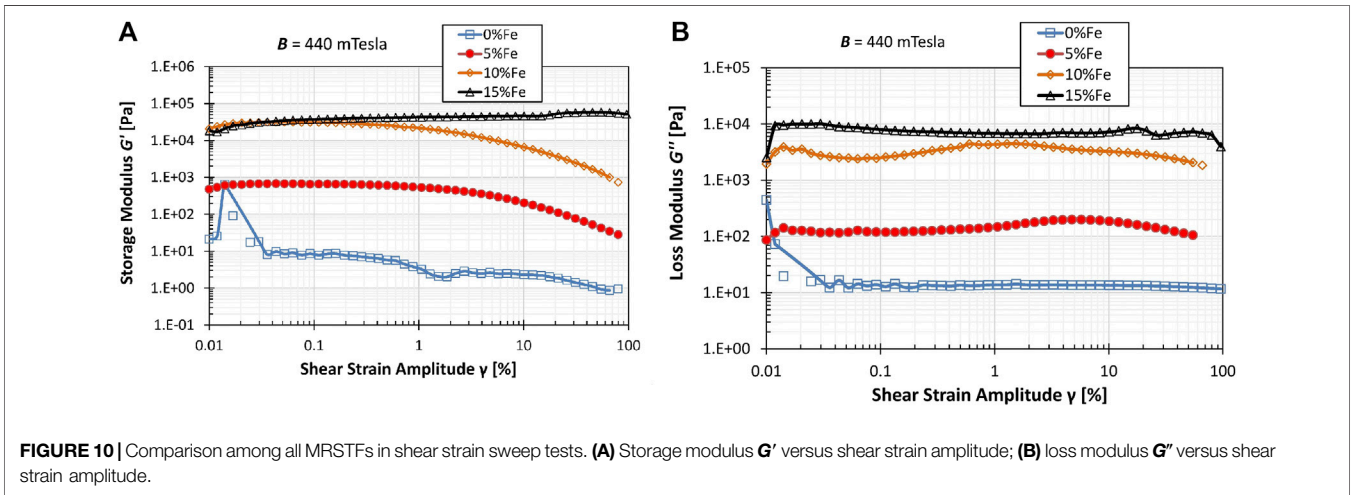
FIGURE 10 | Comparison among all MRSTFs in shear strain sweep tests. **(A)** Storage modulus *G′* versus shear strain amplitude; **(B)** loss modulus *G″* versus shear strain amplitude.

FIGURE 11 | Comparison among all MRSTFs in frequency sweep tests. **(A)** Storage modulus *G′* versus frequency; **(B)** loss modulus *G″* versus frequency.

In **Figures 10** and **11**, at 440 mTesla magnetic field, the MRSTF with higher iron concentration show higher storage and loss moduli, which is due to the contribution of iron in MRSTFs. As shown in **Figure 11**, it is noted that in frequency sweep at 440 mTesla, the storage modulus of all MRSTFs has an increase trend and the sample with lower iron concentration has a larger increase. For loss modulus, the graphs for 0% Fe and 5% Fe show an increase after the 1 Hz frequency, and the increase is weaker in the sample with 5% Fe. With the higher iron centration, the 10% Fe and 15% Fe do not show any increase in loss modulus. At other magnetic fields, the comparisons among all samples also have similar trends.
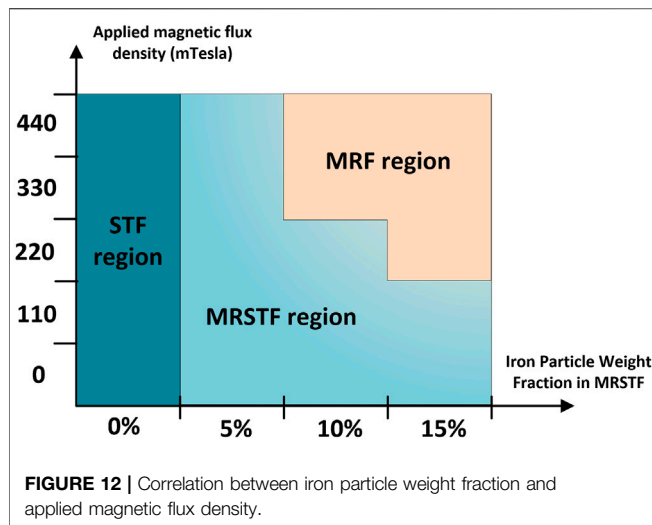
FIGURE 12 | Correlation between iron particle weight fraction and applied magnetic flux density.

Figure 12 summarizes and presents the behavior of MRSTF with various iron particles at different weight concentrations (0, 5, 10, and 15%) and under different magnetic flex densities (0, 110, 220, 330, and 440 mTesla).

For the MRSTFs, they can behave in three different regions, namely, STF region, MRSTF region and MRF region. In STF region, it only shows shear thickening effect and the MR effect does not exist. It can be clearly observed that the MRSTF with zero iron content is in the STF region. With the increase of iron concentration in MRSTFs, they experience both shear thickening phenomenon and MR effect when neither of the iron concentration nor applied magnetic field has high values. It is worthy to state that with the increase of either iron centration or applied magnetic field, the MRSTFs behave closer to the MRF and show lower shear thickening effect. In the MRSTF region, the MRSTFs can be controlled by both magnetic field and applied shear rate. When both the iron concentration and the magnetic field reach high values, the MRSTF behave in the MRF region, where the shear thickening effect diminishes with only presence of MR effect, so the viscosity of the fluids depends purely on the strength of the applied magnetic field.

It can be predicted that for the MRSTF with the iron concentration higher than 15wt%, the boundary of MRF region and MRSTF region will be at lower magnetic field than the 15% Fe MRSTF. Similarly, if the 5% Fe MRSTF is under the magnetic field much stronger than 440 mTesla, the transition from the MRSTF region to the MRF region will occur. The three regions can be used as a guideline on the design of MRSTF, which will benefit the applications of MRSTF as well.

REFERENCES

Avila, A. F., de Oliveira, A. M., Leão, S. G., and Martin, M. G. (2018). Aramid fabric/ nano-size dual phase shear thickening fluid composites response to ballistic impact. *Compos. Part A-Appl. S.* 112, 468–474. doi:10.1016/j.compositesa.2018.07.006

CONCLUSION

In this study, the MRSTFs with different iron concentrations were fabricated from the base STF, and their rheological properties were measured with a rheometer in different types of tests. The results show that both storage and loss moduli of MRSTFs correlate and increase each time when stronger magnetic field is applied. This proves the MR effect of MRSTF. The experimental results also show that when the applied magnetic field was not strong enough, the shear thickening effect can be observed in the MRSTFs. With the flux density of the applied magnetic field raised, the MRSTF behaved with a clear MR effect. It means the viscosity of the MRSTFs can be controlled by both magnetic field and shear rate. The concentration of iron particles also played an important role in the rheological properties of MRSTFs. The sample with higher iron particle concentration showed a lower shear thickening effect but higher MR effect, which means the MRSTF with higher iron concentration can be treated as an effective MR fluid. Meanwhile, the MRSTF with low iron concentration can show good shear thickening effect under weak magnetic field. In strain amplitude sweep tests, when strain amplitude further increases past the critical rate, a slight decrease in both storage and loss moduli was observed. For the oscillatory frequency tests, similar increases in storage and loss moduli were observed, with the increase in magnetic fields. For the frequency increase beyond the critical frequency, slight increases of both moduli were recorded. Three regions of the MRSTF's behavior were proposed to provide the guideline to design the MRSTFs and contribute to their applications.

DATA AVAILABILITY STATEMENT

The raw data supporting the conclusions of this article will be made available by the authors, without undue reservation.

AUTHOR CONTRIBUTIONS

TT, JD, and WL designed the experiments. VS fabricated the MRSTF, conducted the measurements, and analysed the experimental data. All authors contributed to the article and approved the submitted version.

ACKNOWLEDGMENTS

Chen, D. C., and Chen, L. R. (2020). Application of the Taguchi method for finite element analysis of a shear-type magnetorheological fluid damper. *Adv. Mech. Eng.* 12, 1–11. doi:10.1177/1687814019900397

Chen, Q., Liu, M., Xuan, S., Jiang, W., Cao, S., and Gong, X. (2017). Shear dependent electrical property of conductive shear thickening fluid. *Mater. Des.* 121, 92–100. doi:10.1016/j.matdes.2017.02.056

Cossa, K. N. (2019). Basic concepts on rheology and application of shear thickening fluids in protective gear. *SN Appl. Sci.* 1, 1284. doi:10.1007/s42452-019-1315-5

Ding, J., Li, W. H., and Shen, S. Z. (2011). Research and applications of shear thickening fluids. *Recent Pat. Mater. Sci.* 4, 43–49. doi:10.2174/1874464811104010043

Ding, J., Tian, T., Meng, Q., Guo, Z., Li, W., Zhang, P., et al. (2013) Smart multifunctional fluids for lithium ion batteries: enhanced rate performance and intrinsic mechanical protection. *Sci. Rep.* 3, 2485. doi:10.1038/srep02485

Dong, C., Miao, Y., Mi, Z., Song, Q., and Jie, F. (2016). Carbonyl iron powder surface modification of magnetorheological elastomers for vibration absorbing application. *Smart Mater. Struct.* 25, 115005. doi:10.1088/0964-1726/25/11/115005

Grover, G., Verma, S. K., Thakur, A., Biswas, I., and Bhatacharjee, D. (2020). The effect of particle size and concentration on the ballistic resistance of different shear thickening fluids. *Mater. Today* 28, 1472–1476. doi:10.1016/j.matpr.2020.04.823

Han, W., Zhao, T., and Wang, X. (2016). Steady shear viscosity and oscillatory complex viscosity of poly(p-phenylene terephthalamide) solutions in sulfuric acid. *Rheol Acta* 55, 257–266. doi:10.1007/s00397-016-0918-7

Hou, S., and Liu, G. (2020). Research on theoretical modelling and parameter sensitivity of a single-rod double-cylinder and double-coil magnetorheological damper. *Math. Probl. Eng.* 2020, 5489896. doi:10.1155/2020/5489896

Hua, D., Liu, X., Sun, S., Sotelo, M. A., Li, Z., and Li, W. H. (2020). A magnetorheological fluid filled soft crawling robot with magnetic actuation, *IEEE-ASME T. Mech.* 10. doi:10.1109/TMECH.2020.2988049

Li, X., Cao, H. L., Gao, S., Pan, F. Y., Weng, L. Q., Song, S. H., et al. (2008). Preparation of body armour material of Kevlar fabric treated with colloidal silica nanocomposite. *Plast. Rubber Compos.* 37, 223–226. doi:10.1179/174328908X309439

Majumdar, A., Laha, A., Bhattacharjee, D., and Biswas, I. (2017). Tuning the structure of 3D woven aramid fabrics reinforced with shear thickening fluid for developing soft body armour. *Compos. Struct.* 178, 415–425. doi:10.1016/j.compstruct.2017.07.018

Petel, O. E., Ouellet, S., Loiseau, J., Frost, D. L., and Higgins, A. J. (2015). A comparison of the ballistic performance of shear thickening fluids based on particle strength and volume fraction. *Int. J. Impact Eng.* 85, 83–96. doi:10.1016/j.ijimpeng.2015.06.004

Peters, I. R., Majumdar, S., and Jaeger, H. M. (2016). Direct observation of dynamic shear jamming in dense suspensions. *Nature* 532, 214. doi:10.1038/nature17167

Tian, T. (2014). *Study of shear thickening/stiffened materials and their applications, PhD thesis*, University of Wollongong

Wagner, J. W., and Wetzel, E. D. (2007). *Advanced body armor utilizing shear thickening fluids*. U.S. Patent No 7498276B2. Washington, DC: U.S. Patent and Trademark Office.

White, E., Chellamuntu, M, and Rhotstein, J. (2010). Extensional rheology of a shear-thickening cornstarch and water suspension. *Reol. Acta* 49, 119–129. doi:10.1007/s00397-009-0415-3

Yang, J., Sun, S., Li, W., Du, H., Alici, G., and Nakano, M. (2015). Development of a linear damper working with magnetorheological shear thickening fluids. *J. Intel. Mat. Syst. Str.* 26, 1811–1817. doi:10.1177/1045389X15577653

Zhang, X. Z., Li, W. H., and Gong, X. L. (2008). Study on magnetorheological shear thickening fluid. *Smart Mater. Struct.* 17, 015051. doi:10.1088/0964-1726/17/1/015051

Zhang, X. Z., Li, W. H., and Gong, X. L. (2010). Thixotropy of MR shear-thickening fluids. *Smart Mater. Struct.* 19, 125012. doi:10.1088/0964-1726/19/12/125012

Zhou, H., Yan, L., Jiang, W., Xuan, S., and Gong, X. (2016). Shear thickening fluid–based energy-free damper: design and dynamic characteristics. *J. Intel. Mat. Syst. Str.* 27, 208–220. doi:10.1177/1045389x14563869